



Published in final edited form as:

ACS Infect Dis. 2021 February 12; 7(2): 493–505. doi:10.1021/acscinfecdis.0c00869.

Synthesis of Fusidic Acid Derivatives Yields a Potent Antibiotic with an Improved Resistance Profile

Martin Garcia Chavez,

Department of Chemistry, University of Illinois at Urbana–Champaign, Urbana, Illinois 61801, United States; Carl R. Woese Institute for Genomic Biology, University of Illinois at Urbana–Champaign, Urbana, Illinois 61801, United States

Alfredo Garcia,

Department of Chemistry, University of Illinois at Urbana–Champaign, Urbana, Illinois 61801, United States; Carl R. Woese Institute for Genomic Biology, University of Illinois at Urbana–Champaign, Urbana, Illinois 61801, United States

Hyang Yeon Lee,

Department of Chemistry, University of Illinois at Urbana–Champaign, Urbana, Illinois 61801, United States; Carl R. Woese Institute for Genomic Biology, University of Illinois at Urbana–Champaign, Urbana, Illinois 61801, United States

Gee W. Lau,

Department of Pathobiology, College of Veterinary Medicine, University of Illinois at Urbana–Champaign, Urbana, Illinois 61801, United States;

Erica N. Parker,

Department of Chemistry, University of Illinois at Urbana–Champaign, Urbana, Illinois 61801, United States; Carl R. Woese Institute for Genomic Biology, University of Illinois at Urbana–Champaign, Urbana, Illinois 61801, United States

Kailey E. Komnick,

Department of Chemistry, University of Illinois at Urbana–Champaign, Urbana, Illinois 61801, United States; Carl R. Woese Institute for Genomic Biology, University of Illinois at Urbana–Champaign, Urbana, Illinois 61801, United States

Paul J. Hergenrother

Corresponding Author: Paul J. Hergenrother – Department of Chemistry, University of Illinois at Urbana–Champaign, Urbana, Illinois 61801, United States; Carl R. Woese Institute for Genomic Biology, University of Illinois at Urbana–Champaign, Urbana, Illinois 61801, United States; hergenro@illinois.edu.

Supporting Information

The Supporting Information is available free of charge at <https://pubs.acs.org/doi/10.1021/acscinfecdis.0c00869>.

Tables S1–S6, MIC values for FA and equipotent analogues in *S. aureus* in 50% human serum, stability to mouse liver microsomes, IC50 in human foreskin fibroblast-1 cells, list of antibiotics and associated reference numbers with clinically relevant levels of resistance in *S. aureus* and *E. faecium*, antimicrobial assessment of FA, vancomycin, and FA-CP in panel of multidrug-resistant clinical isolates of *S. aureus*, and antimicrobial assessment of FA, vancomycin, and FA-CP in panel of multidrug-resistant clinical isolates of *E. faecium*. Synthetic procedures and characterization for core and side chain derivatives of FA (PDF)

Complete contact information is available at: <https://pubs.acs.org/10.1021/acscinfecdis.0c00869>

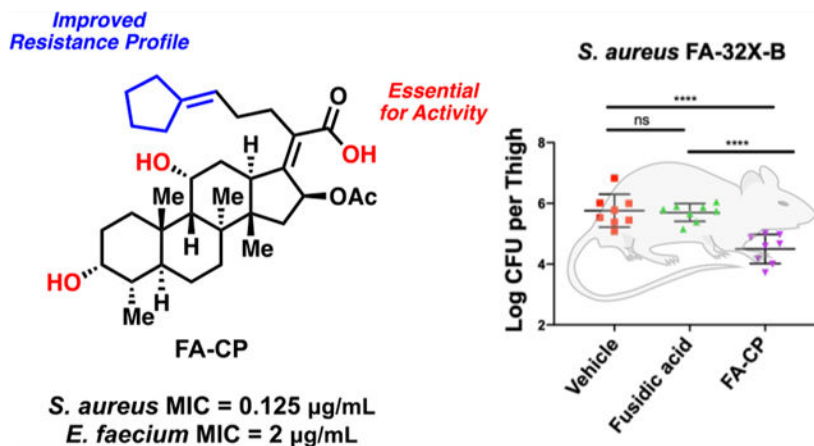
The authors declare the following competing financial interest(s): The University of Illinois has filed patents on some of the compounds described in this manuscript.

Department of Chemistry, University of Illinois at Urbana–Champaign, Urbana, Illinois 61801, United States; Carl R. Woese Institute for Genomic Biology, University of Illinois at Urbana–Champaign, Urbana, Illinois 61801, United States;

Abstract

Fusidic acid (FA) is a potent steroidal antibiotic that has been used in Europe for more than 60 years to treat a variety of infections caused by Gram-positive pathogens. Despite its clinical success, FA requires significantly elevated dosing (3 g on the first day, 1.2 g on subsequent days) to minimize resistance, as FA displays a high resistance frequency, and a large shift in minimum inhibitory concentration is observed for resistant bacteria. Despite efforts to improve on these aspects, all previously constructed derivatives of FA have worse antibacterial activity against Gram-positive bacteria than the parent natural product. Here, we report the creation of a novel FA analogue that has equivalent potency against clinical isolates of *Staphylococcus aureus* (*S. aureus*) and *Enterococcus faecium* (*E. faecium*) as well as an improved resistance profile *in vitro* when compared to FA. Importantly, this new compound displays efficacy against an FA-resistant strain of *S. aureus* in a soft-tissue murine infection model. This work delineates the structural features of FA necessary for potent antibiotic activity and demonstrates that the resistance profile can be improved for this scaffold and target.

Graphical Abstract



Keywords

antibiotics; fusidic acid analogues; resistance profile; *in vivo* efficacy; EF-G inhibitor

Recent reports have confirmed that the worrisome rise of antibiotic-resistant bacterial infections is continuing.^{1,2} Some of the most problematic Gram-positive pathogens are methicillin-resistant *Staphylococcus aureus* (MRSA) and vancomycin-resistant *Enterococci* (VRE), and accordingly, these have been classified as serious threats by the Centers for Disease Control and Prevention (CDC).³ The emergence of bacteria resistant to vancomycin,⁴ a drug of last resort against Gram-positive infections, highlights the need to develop or re-engineer drugs that could be efficacious against these problematic pathogens.

Fusidic acid (**1**, Figure 1) is a steroidal antibiotic that is produced by the fungus *Fusidium coccineum*.⁵ Its mechanism of action involves inhibition of protein synthesis by stabilizing the elongation factor G (EF-G) complex, resulting in the truncation of peptide elongation.⁶ EF-G being an unusual antibacterial target likely minimizes the cross-resistance of FA with other antibiotics.⁷ FA is a Gram-positive-only antibiotic that has been used since the 1960s in Europe to treat Gram-positive infections and has been particularly effective in treating MRSA.^{7,8} To date, FA is approved in 23 countries and is administered via oral, intravenous, and topical routes.⁷ In the United States, FA has achieved its primary and secondary efficacy end points in phase 3 clinical trials for the treatment of patients with acute bacterial skin and skin structure infections (ABSSSI).⁹ FA has also received Orphan Drug Designation from the Food and Drug Administration (FDA) for the treatment of prosthetic joint infections and gained Qualified Infectious Disease Product Designation under the Generating Antibiotic Incentives Now (GAIN) Act.¹⁰ Strikingly, an analysis conducted in 2011 showed that virtually all (99.7%) of *S. aureus* strains in the United States were susceptible to FA.⁷

Despite the clinical success of FA, the high resistance frequency in the range of 1×10^{-6} to 1×10^{-8} at 2–16X the minimum inhibitory concentration (MIC) coupled with drastic MIC shifts upon resistance remain a major concern and are a hindrance to its wider usage.⁷ FA-resistant bacterial strains display a varied profile, illustrated by the heterogeneity in mutations observed in the laboratory and in the clinic.¹¹ Some of the most prevalent mutations in the *fusA* gene (encoding EF-G) observed in the clinic are V90L, H457Q, L461K, and A655V.⁷ Especially concerning is the L461K mutation, observed clinically in *S. aureus* strains resistant to FA, which leads to MIC values of $>256 \mu\text{g/mL}$, a >2048 -fold increase in MIC upon resistance.⁷ This large shift in MIC upon resistance observed from a single amino acid mutation is consistent with the hypothesis that single enzyme inhibitors are more prone to display elevated shifts in MIC upon resistance relative to antibiotics with multiple targets.^{12,13} In addition to mutations in the *fusA* gene, another source of clinical resistance for FA is the overexpression of the FusB family of proteins encoded by the *fusB* gene usually carried on a 21-kb plasmid (pUB101); FusB binds to EF-G and drives the dissociation of FA from its target.¹⁴ More recently, *fusC* and *fusD* genes have also been discovered in clinical isolates of *S. aureus*.¹⁵ The *fusC* gene has been associated with driving resistance in *S. aureus* and coagulase-negative staphylococci, while the *fusD* gene has been linked to conferring resistance among *Staphylococcus saprophyticus*.¹⁵

The aforementioned resistance challenges necessitate a front-loading dosing regimen, with 3 g of FA taken on the first day of treatment and 1.2 g taken daily thereafter, allowing for considerable drug plasma levels to be reached (C_{max} of greater than $130 \mu\text{g/mL}$ in patients).⁷ Despite multiple efforts to construct FA analogues,^{16–32} none of these derivatives are as active as FA against Gram-positive pathogens;⁷ in addition, none of them improve on the resistance issues noted above. No FA derivatives have gained traction translationally, and only FA itself has moved forward to the clinic from this antibiotic class. While no FA derivatives with improved activity against Gram-positive bacteria have been reported, derivatives with improved activity relative to FA have been reported against the malaria parasite *Plasmodium falciparum*.^{21,26,30}

Notable challenges in constructing FA variants through direct modification of this natural product include the presence of reactive functional groups such as the olefinic side chain, an α,β -unsaturated carboxylic acid, an acetate, and two sterically hindered alcohols (Figure 1). Furthermore, the unique chair–boat–chair core conformation of FA makes the total synthesis of this antibiotic challenging, and such routes are not yet suitable for the rapid generation of derivatives.^{24,25,33} Intrigued by the translational potential of FA, here we report the development of synthetic routes from FA that provide rapid access to novel variants with modified side chains, leading to the discovery of a novel FA analogue with an improved resistance profile.

RESULTS

Synthesis and Antibacterial Assessment of FA Derivatives Where the Carboxylic Acid and Alcohols Are Modified.

Key to this study was to first determine the important structural features necessary to retain the potent antibacterial activity of FA. Although FA derivatives have been reported in the literature,^{16–32} a systematic antimicrobial activity assessment of FA derivatives with MIC values against key Gram-positive pathogens does not exist. Thus, as a prelude to our work, we first synthesized several known FA analogues and assessed their antibacterial activity, with the specific goals of probing the importance of the carboxylic acid and alcohols.

The role of the carboxylic acid was investigated via construction of ester **2** and amide **3**, using previously published routes (Figure 2A).^{26,27} Diketone **4** was synthesized previously using the Jones oxidation reaction.³⁴ Herein, diketone **4** was synthesized using pyridinium chlorochromate (Figure 2A). Oxidation solely at C3 was effected using recently published conditions to provide compound **5** (Figure 2A).²⁸ The monoketone at C11 was previously synthesized by treating FA with Kiliani's reagent in a low yielding process.²⁹ Herein, a five-step sequence was developed to generate the C11 ketone (Figure 2B). This route required the protection of the carboxylic acid to generate intermediate **6**.^{21,23} The steric hindrance at the C11 position induced by 1,3-diaxial interactions was leveraged, and the C3 alcohol was selectively protected with TBS to generate **7**. The C11 alcohol was then oxidized with pyridinium chlorochromate to generate **8**. Removal of the TBS protecting group in compound **8** with aqueous hydrofluoric acid provided **9**, and subsequent deprotection of the pivaloyloxymethyl protecting group under mild basic conditions afforded the target monoketone, compound **10** (Figure 2B). Key to this work was utilizing a suitable protecting group for the carboxylic acid that could be removed under mild basic conditions, as lactonization between the C16 acetyl and the C21 carboxylic acid occurs under strongly basic conditions.^{21,23} Accordingly, POM-Cl, used previously to protect the FA carboxylic acid,^{21,23} was utilized to protect the carboxylic acid as a pivaloyloxy-methyl ester based on its ability to be removed under mild conditions.^{21,23}

Antibacterial activity of FA analogues **2–5** and **10** was assessed against *S. aureus* ATCC 29213 using standard MIC assays following Clinical and Laboratory Standards Institute (CLSI) guidelines.³⁵ As shown in Figure 2, FA analogues **2–4** display significantly reduced antibacterial activity, reinforcing the importance of the free carboxylic acid and both of

the alcohols. Oxidation of the secondary alcohols separately is more tolerated, with the monoketones at C3 (compound **5**) and at C11 (compound **10**) having MIC values only 4–8-fold worse than FA (Figure 2).

Synthesis and Antibacterial Evaluation of Side Chain Analogues.

As modifications to FA shown in Figure 2 were all deleterious to antibacterial activity, the focus shifted to modifications of the *gem*-dimethyl alkene side chain. This work was informed by the crystal structure of the ribosome trapped with EF-G in a post-translocational state with FA bound;³⁶ this complex indicates that the side chain of FA is positioned in a large, hydrophobic pocket of EF-G.³⁶

Several FA analogues with modifications to the side chain have been previously reported, such as derivatives where the C24 and C25 or the C17 and C20 double bonds have been reduced.^{17,22} Furthermore, truncation of the C26 and C27 methyl groups has also been reported as well as analogues where the C26 and C27 methyl groups were modified via microbial oxidation.^{37,38} Heteroatoms have also been introduced via ozonolysis of the C24 and C25 double bond.¹⁸ Aryl side chain analogues of FA have also been synthesized and used to conduct photolabeling studies.²³ Notably, all of the previously reported side chain analogues of FA have reduced antibacterial activity relative to FA.

To provide access to FA derivatives with novel side chains, a modular synthetic route for rapid generation of a variety of compounds with modified side chains was envisioned. Aldehyde **11**, generated previously by ozonolysis²³ and herein via dihydroxylation followed by oxidative cleavage (Figure 3A), was selected as the pluripotent intermediate that could be transformed via olefinations, one-carbon homologations, and cross-metathesis reactions to the various analogues. Using **11**, halogens were introduced via a one-carbon homologation reaction with carbon tetrachloride, carbon tetrabromide, and carbon tetraiodide, respectively, to generate intermediates **12–14** (Figure 3B). Subsequent deprotection with potassium carbonate in methanol afforded novel halogenated compounds **15–17** (Figure 3B). Construction of the analogous fluorinated compound was accomplished by treating aldehyde **11** with chlorodifluoroacetic acid and triphenylphosphine at elevated temperatures to generate **18** and deprotection to generate difluorinated derivative **19** (Figure 3C). Aldehyde **11** was also converted to olefin **20** and fully deprotected to generate **21** as previously reported (Figure 3D).³⁷

Olefin **20** was used as another key point of diversity and divergence to generate compounds containing symmetrical side chains with the C24 and C25 double bond intact. Thus, to form cyclic derivatives, olefin **20** was coupled via a cross-metathesis reaction with methylenecyclopentane, methylenecyclohexane, and 4-methylenetetrahydropyran using Grubbs' catalyst 2 to generate analogues **22–24**. Deprotection generated novel cyclic side chain derivatives **25–27** (Figure 3E). Lastly, compound **28** with a fully saturated side chain was synthesized as previously reported using Lindlar's catalyst (Figure 3F).²²

With this collection of FA derivatives in hand, the MIC of each compound against *S. aureus* was determined (Figure 3). Compounds **15**, **17**, **19**, **21**, and **28** displayed modest decreases in potency relative to FA. Notably, analogues **16**, **25** (hereafter referred to as FA-CP), **26**, and

27 displayed equipotent activity to FA, suggesting the antibiotic potential of FA derivatives with modified side chains (Figure 3).

Evaluation of Resistance Frequency of Equipotent Analogues of FA.

The resistance frequency of the equipotent analogues (**16**, **25** (FA-CP), **26**, and **27**) was assessed in head-to-head experiments with FA. The large inoculum method was used in order to generate resistance mutants and derive the resistance frequency of FA and the equipotent analogues.³⁹ The resistance frequency was determined at 2, 4, 8, 16, and 32X the MIC, which is 0.125 $\mu\text{g}/\text{mL}$ for all compounds. The resistance frequency at the listed MICs was then compared head-to-head against FA, and statistical significance was then determined using one-way ANOVA with Tukey's multiple comparisons. As shown in Figure 4A,B, compounds FA-CP and **26** displayed an improvement in resistance frequency relative to FA. FA-CP displayed a modest improvement in resistance frequency at 2 and 32X the MIC, while analogue **26** only displayed an improvement at 32X the MIC (Figure 4A,B). This is in contrast with analogues **16** and **27**, which displayed a worse resistance frequency relative to FA (Figure 4C,D).

Effect of Human Serum Binding, Assessment of Metabolic Stability, and Mammalian Cell Toxicity.

The translational potential of the novel derivatives was further investigated by assessing parameters important in antibacterial development, such as the effect of human serum binding, metabolic stability, and mammalian cell toxicity. FA is reported to be highly protein bound, with human plasma protein binding of 97%.⁴⁰ Additionally, the MIC for FA when 50% human serum is included in the media shifts to 16–256X higher.⁴⁰ In this work, the shift in MIC for *S. aureus* in 50% human serum was determined to be very similar for FA as compared to compounds **16**, FA-CP, **26**, and **27** (Table S1). In addition, the stability of the novel derivatives to mouse liver microsomes was similar to FA (Table S2). FA, **16**, FA-CP, **26**, and **27** exhibited low toxicity toward human foreskin fibroblast-1 cells (HFF-1), with all compounds giving IC_{50} values greater than 50 μM (Table S3).

Mode-of-Action of Novel FA Derivative.

FA-CP was selected for additional studies investigating the mode-of-action. For these studies, resistance mutants were generated at 32X the MIC of FA-CP and FA, and sequencing of the *fusA* gene (coding for EF-G, the target of FA) revealed mutations in *fusA*, suggesting that FA-CP engages the same target as FA. Specifically, for FA and FA-CP, the *fusA* gene was sequenced for 40 different resistant colonies generated at 32X the MIC, 20 colonies for each compound. As shown in Table 1, the resistance mutants observed for FA are in accord with those seen previously in analogous studies. Specifically, mutations F88L,^{11,41} T436I,^{11,41} H457N,⁴¹ and D434N¹¹ have been identified in bacterial cell culture studies with *S. aureus* and FA. Additionally, H457Y^{11,41–44} has been observed in bacterial cell culture studies as well as clinical isolates of *S. aureus* that are resistant to FA. Consistent with the notion that FA-CP engages the same target as FA, single amino acid substitutions (H457Y, D434N, and F88L) within EF-G were found in the 20 different FA-CP colonies (Table 1).

The MICs of FA and FA-CP against these resistance mutants were also determined, and it was found that the mutants generated from FA-CP typically displayed a reduced shift in MIC upon resistance relative to the mutants generated from FA (Table 1). Specifically, the highest MIC observed for colonies generated from FA-CP was 64 $\mu\text{g}/\text{mL}$ (fold increase from wild-type (WT) *S. aureus*: 512) (Table 1). In our in-house studies, the highest MIC observed for FA was 256 $\mu\text{g}/\text{mL}$ (fold increase from WT *S. aureus*: 2048) (Table 1).

In a separate experiment, *S. aureus* strains resistant to FA were generated at 4, 8, 16, and 32X the MIC. Mutations found in the *fusA* gene of the resistant colonies are consistent with what has been observed in previous studies conducted with FA. Specifically, observed mutations in the *fusA* gene causing single amino acid substitutions, T385N,⁴⁵ R464L,¹¹ F88L,^{11,41} H457L,⁴¹ T436I,^{11,41} H457N,⁴¹ and D434N,¹¹ have been identified in bacterial cell culture studies with *S. aureus* and FA. Furthermore, H457Y^{11,41-44} and P406L^{11,41,42,45} have been observed in bacterial cell culture studies as well as clinical isolates of *S. aureus* that are resistant to FA. FA-CP was evaluated against these 11 FA-resistant strains for antimicrobial activity. Although FA-CP displays cross-resistance with FA, expected as the target is conserved between the two compounds, FA-CP displays a 2–8-fold improvement in activity against these FA-resistant strains relative to FA (Table 2).

Activity of FA-CP and FA against Multidrug-Resistant Clinical Isolates of *S. aureus*, *E. faecium*, and an *S. aureus* Strain Harboring the *fusC* Gene.

The activity of FA, FA-CP, and vancomycin was assessed against 29 different clinical isolates of *S. aureus*. FA and FA-CP displayed no cross-resistance with vancomycin and retained potent activity against the 29 different clinical isolates assessed (Figure 5A). Noteworthy is that within this collection of clinical isolates, there are strains with resistance to a wide variety of antibiotics, including cefoxitin, clindamycin, doxycycline, erythromycin, gentamicin, levofloxacin, oxacillin, penicillin, tetracycline, and trimethoprim/sulfamethoxazole (see Tables S4 and S5 for a full list of resistance profiles).

The activity of FA and FA-CP was also assessed against a *S. aureus* strain that possesses the *fusC* gene, strain *S. aureus* ATCC BAA-1721.⁴⁶ FA-CP displayed cross-resistance with FA, as both compounds displayed an MIC of 8 $\mu\text{g}/\text{mL}$ against this strain.

The activity of FA, FA-CP, and vancomycin was also assessed against six different clinical isolates of *E. faecium* (Figure 5B). As a reference point, the MIC of FA and FA-CP against a sensitive strain of *E. faecium* ATCC 19434 is 2 $\mu\text{g}/\text{mL}$ for both antibacterial agents. FA and FA-CP displayed no cross-resistance with vancomycin in the *E. faecium* clinical isolates. Excitingly, FA and FA-CP retained potent activity against VRE with high levels of vancomycin resistance (vancomycin MIC = 512 $\mu\text{g}/\text{mL}$). See Table S6 for a full list of resistance profiles.

Pharmacokinetic Studies and *in vivo* Efficacy of FA and FA-CP.

As a prelude to the mouse infection studies, the tolerability of FA (sodium fusidate) and FA-CP was assessed in mice at 50 mg/kg (intraperitoneal injection, once-a-day for 4 days), and both compounds were well tolerated by mice at this dose. Noteworthy is the rapid metabolism of FA in rodents, which is a major hurdle in the preclinical evaluation of FA

analogues in mouse models.^{28,32} Head-to-head assessment of the pharmacokinetics of FA and FA-CP in mice revealed that these compounds have similar PK profiles (Figure 6A). The mouse and human PK profiles for FA are considerably different, as FA has a long half-life in humans of around 10–14 h,^{7,47} with predominant metabolism by the liver;⁴⁸ the rapid clearance observed in mice could be driven by the formation of 3-epiFA, a metabolite that has not been observed in humans.^{28,32}

Encouraged by the efficacy of FA-CP against the panel of clinical isolates, the lack of toxicity to mammalian cells, and the promising tolerability and pharmacokinetic data, FA-CP was compared head-to-head to FA in *in vivo* efficacy studies; the design of these efficacy studies was guided by mouse models previously conducted with FA.⁴⁹ First, a sensitive strain of *S. aureus* was assessed in a neutropenic thigh infection burden model utilizing *S. aureus* ATCC 29213, in which FA-CP and FA display the same MIC of 0.125 $\mu\text{g}/\text{mL}$. After infection, three doses of FA-CP and FA were administered (50 mg/kg, intraperitoneal injection) 1, 2, and 3 h postinfection to separate groups of mice. Mice were sacrificed 24 h postinfection, and bacterial burden in the thigh muscle tissue homogenates was determined by serial dilution plating onto tryptic soy agar. Significant reductions in bacterial burden were observed with FA and FA-CP (Figure 6B).

The improved potency of FA-CP against FA-resistant strains motivated and guided the second neutropenic thigh infection burden model. An FA-resistant *S. aureus* strain, FA-32X-B, generated at 32X the MIC of FA, was used for this study. FA has an MIC of 32 $\mu\text{g}/\text{mL}$, while FA-CP displays an MIC of 4 $\mu\text{g}/\text{mL}$ (Table 2). After infection, three doses of FA-CP and FA were administered (50 mg/kg, intraperitoneal injection) 1, 2, and 3 h postinfection to separate groups of mice. Mice were sacrificed 8 h postinfection, and bacterial burden in the thigh muscle tissue homogenates was determined by serial dilution plating onto tryptic soy agar. This resulted in reductions in bacterial burden with FA-CP and no efficacy with FA (Figure 6C). This study is, to our knowledge, the first mouse bacterial infection model in which a novel derivative of FA displays improved efficacy relative to FA.

DISCUSSION

Despite FA being approved in Europe since the 1960s to treat problematic *S. aureus* infections, there have been no follow-on drugs, and FA remains the only member of the fusidane class to be used clinically.⁷ The high resistance frequency, drastic shifts in MIC upon bacterial resistance to FA, and lack of effective derivatives have narrowed the development path for this antibiotic class.

A considerable challenge in the creation of new and effective derivatives of FA has been a clouded structure–activity relationship for this compound, due to heterogeneity in the reported biological data for derivatives, with many compounds evaluated against the malaria parasite *Plasmodium falciparum*^{21,26,30} and *Mycobacterium* species^{28,31,32} but not against Gram-positive bacteria. In this work, we have constructed and assessed both previously synthesized derivatives and novel derivatives, allowing for a clearer structure–activity relationship (SAR) to emerge. Most notably, while previous investigations suggested that changes in the hydrophobic side chain of FA diminished antibacterial activity,^{17,18,22,23,37,38}

here we show that certain changes at this position are not only tolerable but lead to derivatives with favorable resistance profiles compared to FA.

Specifically, the reduced shift (relative to that observed for FA) in MIC upon resistance of *S. aureus* to FA-CP is an important feature of this compound. The highest MIC for the resistance mutants generated to FA-CP was 64 $\mu\text{g}/\text{mL}$, versus 256 $\mu\text{g}/\text{mL}$ for resistance mutants generated to FA. In principle, this improvement could allow for administration of less FA-CP or a similar compound. Although FA is considered a safe antibiotic, gastrointestinal side effects have been observed in 30–58% of patients treated with FA, and up to 30% of patients have elevated bilirubin.⁴⁷

Another interesting and potentially useful aspect of FA-CP is the ability of this compound to retain some activity against strains of *S. aureus* that are resistant to FA, including in a mouse model of infection. Specifically, FA-CP displayed *in vivo* efficacy against an FA-resistant *S. aureus* strain generated at 32X the MIC of FA (strain FA-32X-B). Our sequencing studies reveal that FA-32X-B possesses the mutation P406L in the EF-G protein. Noteworthy is the fact that this mutation has not only been observed in bacterial cell culture studies but also been identified in clinical isolates of *S. aureus*,^{11,42} highlighting the potential of FA-CP to retain efficacy *in vivo* against some clinical isolates of *S. aureus* that are resistant to FA.

Sequencing studies also revealed some interesting differences between the mutational profile of bacteria arising from FA versus FA-CP treatment. In our in-house studies, five different amino acid changes were observed in EF-G for FA-resistant *S. aureus*, while only three different amino acid mutations in EF-G were observed for FA-CP-resistant *S. aureus*. Mutations in EF-G have been classified into four different groups based on their role in resistance to FA: Group A (mutations affecting FA binding), Group B (mutations affecting EF-G ribosome interactions), Group C (mutations affecting EF-G conformation), and Group D (mutations affecting EF-G stability).⁵⁰ Moreover, Group A mutations involve amino acids that are in direct contact with FA and with residues that can shape the drug pocket.⁵⁰ Additionally, it has been postulated that Group C mutations are related to the interdomain orientation of EF-G, which can affect the FA-binding pocket along with the conformation dynamics and FA locking of EF-G.⁵⁰ The mutations in FA-resistant strains found in our studies have been previously classified and belong to Group A and Group C, whereas all the mutations observed for FA-CP-resistant strains belong to Group A, indicating that these mutations are in regions that can affect FA binding.

While mutation to *fusA*, the gene encoding for EF-G, is a major mechanism of resistance for FA, it is important to note that other resistance mechanisms are operational in clinical isolates, specifically, the horizontal acquisition of plasmids harboring *fusB* or *fusC*.¹⁵ These resistance genes encode protective proteins that drive the dissociation of the EF-G ribosome complex from FA.⁵¹ Analogous to the shifts in MIC observed for FA upon mutations to the *fusA* gene, an increase in MIC has also been reported in clinical isolates that possess the *fusB* and/or *fusC* genes. For example, MIC ranges of 2–64 $\mu\text{g}/\text{mL}$ in staphylococcal clinical isolates have been reported for clinical isolates that carry the *fusC* gene, and MIC ranges of 4–1024 $\mu\text{g}/\text{mL}$ have been reported for strains that possess the *fusB* gene.^{15,44,46} Due to the clinical relevance of strains that have acquired the *fusC* gene, the MIC of FA-CP

was assessed against a strain that possesses this gene. FA-CP displays the same MIC as FA against *S. aureus* ATCC BAA-1721, with an MIC of 8 $\mu\text{g}/\text{mL}$. While resistance driven by the *fusB* and *fusC* genes is worrisome, the primary mechanism of clinical resistance to FA is still resistance mediated by mutations in the *fusA* gene.^{7,42} Specifically, mutation L461K found in clinical isolates of *S. aureus* is of high concern due its drastic shift in MIC (MIC > 256 $\mu\text{g}/\text{mL}$) upon a single amino acid mutation.⁷ Perhaps even more problematic are clinical isolates of *S. aureus* that are resistant to FA and possess four different EF-G amino acid alterations within the same strain. Five such clinical isolates have been isolated, and they all showed the following alterations in EF-G: V90I, H457Q, L461K, and A655V.⁴² All of these strains have an MIC greater than 256 $\mu\text{g}/\text{mL}$, highlighting the prominent role that mutations to the *fusA* gene play in the development of resistance to FA in the clinic.⁴² It may be possible to design FA derivatives that retain strong binding to these mutant versions of EF-G, and FA derivatives with a further improved resistance profile can also be envisioned.

FA-CP is the first analogue to outperform FA in a mouse infection model, which more broadly suggests the potential for certain FA derivatives. The important improvement in the resistance profile observed for FA-CP has some precedence in antibacterial drug discovery, for example in the dihydrofolate reductase inhibitor iclaprim⁵² and leucyl-tRNA synthetase inhibitor DS86760016,⁵³ with improvement in each case likely due to subtly different modes of target engagement relative to the parent antibiotics (trimethoprim and GSK2251052, respectively). With access to derivatives now facile and the ability to improve upon its resistance profile now demonstrated, novel antibiotics of the fusidane class can be developed for the treatment of a variety of bacterial infections. Finally, as demonstrated by its outstanding activity against permeability defect *Escherichia coli*,⁵⁴ FA has potential against Gram-negative bacteria but is accumulation limited; the detailed SAR reported herein should assist in exploiting this untapped potential of FA to combat drug-resistant Gram-negative infections.

METHODS

Bacterial Strains.

S. aureus ATCC 29213, *E. faecium* ATCC 19434, and *S. aureus* ATCC BAA-1721 were obtained from the American Type Culture Collection (ATCC). Resistant strains of *E. faecium* were obtained from the CDC. Resistant strains of *S. aureus* were obtained from the Network on Antimicrobial Resistance in *Staphylococcus aureus* (NARSA) and the CDC.

Antimicrobial Susceptibility Tests.

Susceptibility testing was performed in biological triplicate, using the microdilution broth method as outlined by CLSI. Bacteria were cultured with cation-adjusted Muller-Hinton broth (Sigma-Aldrich, Cat# 90922) in round-bottom 96-well plates (Corning, Cat# 3788). Human serum (ultrafiltrate, unspecified gender, 30K Dalton membrane filtered) was purchased from BioIVT (Hicksville, NY).

Cell Culture.

HFF-1 cells were obtained from ATCC. HFF-1 cells were grown in DMEM with 15% fetal bovine serum (Gemini Benchmark, Cat# 100–106), 100 $\mu\text{g}/\text{mL}$ of penicillin, and 100 $\mu\text{g}/\text{mL}$ of streptomycin. All cells were cultured at 37 °C in a 5% CO₂ environment. Media was prepared by the University of Illinois School of Chemical Sciences Cell Media Facility.

Cell Viability.

Cells were harvested, seeded in a 96-well plate, and allowed to adhere. Cells were treated with investigational compounds in DMSO (1% final concentration). Cells were incubated for 72 h before viability was assessed by the Alamar Blue Assay. Raptinal (20 μM) was used as a dead control.

Mouse Liver Microsome Stability Assay.

A mixture of PBS (pH 7.4), NADPH regenerating system solution A (Corning Life Sciences), and NADPH regenerating system solution B (Corning Life Sciences) was incubated at 37 °C in a shaking incubator for 5 min. Next, compound was added in DMSO (final concentration 50 μM , 0.5% DMSO) before ice-cold mouse liver microsomes (Thermo Fisher, male CD-1 mice, pooled) were added (final protein concentration of 1 mg/mL). An aliquot was immediately removed, quenched with an equal volume of 100 μM internal standard, and centrifuged at 13 000 rcf for 3 min. The reactions were incubated at 37 °C in a shaking incubator for 3 h. A second aliquot was removed and quenched. Samples were analyzed with the 5500 QTRAP LC-MS/MS system (Sciex, Framingham, MA) in the Metabolomics Laboratory of Roy J. Carver Biotechnology Center, University of Illinois at Urbana–Champaign. Software Analyst 1.6.2 was used for data acquisition and analysis. The 1200 series HPLC system (Agilent Technologies, Santa Clara, CA) includes a degasser, an autosampler, and a binary pump. The LC separation was performed on an Agilent Sb-Aq column (4.6 \times 50 mm, 5 μm) with mobile phase A (0.1% formic acid in water) and mobile phase B (0.1% formic acid in acetonitrile). The flow rate was 0.3 mL/min. The linear gradient was as follows: 0–3 min, 100% A; 10–16 min, 5% A; 16.5–22 min, 100% A. The autosampler was set at 10 °C. The injection volume was 1 μL . Mass spectra were acquired under both positive (ion spray voltage +5500 V) and negative (ion spray voltage –4500 V) electrospray ionization (ESI). The source temperature was 450 °C. The curtain gas, ion source gas 1, and ion source gas 2 were 33, 65, and 60 psi, respectively. Multiple reaction monitoring (MRM) was used for quantitation.

Selection of Resistant Mutants.

Resistant mutants were selected via the large inoculum method. Briefly, *S. aureus* ATCC 29213 (1×10^9 CFU) was plated on 100 mm plates of LB agar containing 4, 2, 1, 0.5, and 0.25 $\mu\text{g}/\text{mL}$. Colonies were visible after incubation at 37 °C for 24 h. Resistant colonies were confirmed by streaking on selective media with the same concentration of fusidic acid and compounds **16**, FA-CP (**25**), **26**, **27**.

Sequencing of *fusA*.

FusA was amplified by colony polymerase chain reaction (PCR). Colonies were picked and diluted in 100 μL of sterile H_2O . PCR reactions are set up by combining MiFi Mix (Bioline, London, UK), 20 μM primer mix [*fusA*-F2, *fusA*_seq1, forward EF-G2, and reverse EF-G] (*S. aureus* ATCC 29213), template DNA, and H_2O . Reactions were performed on a C1000 Thermal Cycler (Bio-Rad, Hercules, CA) with the following conditions: 5 min of denaturation at 95 $^\circ\text{C}$, followed by 30 cycles of 20 s at 95 $^\circ\text{C}$, 20 s at 50 $^\circ\text{C}$, and either 1 min (*fusA1*) or 1.5 min (*fusA2*) at 72 $^\circ\text{C}$. A 10 μL portion of the PCR reaction mixture was analyzed by agarose gel to confirm the product. PCR reactions were purified using GeneJET PCR Purification Kit (Thermo Scientific). PCR amplicons were submitted to the Core DNA Sequencing Facility at the University of Illinois at Urbana–Champaign for Sanger sequencing with the following primers to sequence the *fusA* [*fusA2*, *fusA*_seq1, forward EF-G2, forward EF-G3, forward EF-G4]. See the Supporting Information to find the sequence of the primers used in this study.

Mouse Maximum Tolerated Dose (MTD) of Sodium Fusidate and FA-CP (25).

The protocol was approved by the Institutional Animal Care and Use Committee (IACUC) at the University of Illinois at Urbana–Champaign (protocol number: 16144 and 19181). In these studies, 10- to 12-week-old female C57BL/6 mice purchased from Charles River were used. The maximum tolerated dose (MTD) of a single compound was determined first. Sodium fusidate and FA-CP (25) were formulated in 5% DMSO, 10% Tween 20, and 85% PBS. Sodium fusidate and FA-CP (25) were given by intraperitoneal (IP) injection. All the mice were monitored for signs of toxicity for 2 weeks. For multiple doses, the compound was given by daily IP injection for 4 consecutive days, and mice were monitored for signs of toxicity for 1 month. The MTD was the highest dosage with acceptable toxicity (e.g., < 20% weight loss). Sodium fusidate and FA-CP (25) were well tolerated as a single dose of 50 mg/kg. Further analysis showed that sodium fusidate and FA-CP (25) were well tolerated with daily dosing of 50 mg/kg for 4 consecutive days. The MTD of FA-CP (25) was used to inform the dosing schedule used in subsequent efficacy studies.

Pharmacokinetic Assessment of Sodium Fusidate and FA-CP (25).

The protocol was approved by the IACUC at the University of Illinois at Urbana–Champaign (protocol number: 16144, 19181). In these studies, 10- to 12-week-old female C57BL/6 mice purchased from Charles River were used. The compounds were formulated in 5% DMSO, 10% Tween 20, and 85% PBS. Mice were treated with sodium fusidate or FA-CP (25) (50 mg/kg) via IP injection with three mice per time point (15, 30, 45, 60, 120, and 240 min). At specific time points, mice were sacrificed, blood was collected and centrifuged, and the serum was frozen at $-80\text{ }^\circ\text{C}$ until analysis. The proteins in a 10 μL aliquot of serum were precipitated by the addition of 50 μL of acetonitrile with the addition of 10 μL of 1.6 $\mu\text{g}/\text{mL}$ of internal standard (sodium fusidate was the internal standard when measuring FA-CP (25), and FA-CP (25) was the internal standard when measuring sodium fusidate). The sample was then vortexed and centrifuged to remove the proteins. Supernatants were analyzed with the QTRAP 5500 LC-MS/MS system (Sciex) in the Metabolomics Laboratory of the Roy J. Carver Biotechnology Center, University of Illinois at Urbana–Champaign.

Software Analyst 1.6.2 was used for data acquisition and analysis. The 1200 Series HPLC System (Agilent Technologies) includes a degasser, an autosampler, and a binary pump. The LC separation was performed on an Agilent Zorbax SB-Aq column (4.6 × 50 mm; 5 μm) with mobile phase A (0.1% formic acid in water) and mobile phase B (0.1% formic acid in acetonitrile). The flow rate was 0.3 mL/min. The linear gradient was as follows: 0–1 min, 95% A; 8–13 min, 0% A; 8.1–18.5 min, 95% A. The autosampler was set at 10 °C. The injection volume was 5 μL. Mass spectra were acquired under negative electrospray ionization with a voltage of –4500 V. The source temperature was 450 °C. The curtain gas, ion source gas 1, and ion source gas 2 were 32, 60, and 60 psi, respectively. MRM was used for quantitation: fusidic acid: *m/z* 515.3 → 393.3, FA-CP (**25**): *m/z* 541.4 → 437.2. The limit of quantitation of (S/N = 10) was 1 nM. Pharmacokinetic parameters were calculated with a one-compartment model using a nonlinear regression program (Phoenix WinNonlin Version 8.1; Certara USA).

Neutropenic Thigh Infection Burden Study with Sodium Fusidate and FA-CP (**25**).

Mouse studies were carried out in strict accordance with the recommendations in the guide for the Care and Use of Laboratory Animals of the National Institutes of Health. The animal protocol was approved by the IACUC at the University of Illinois at Urbana–Champaign (protocol number: 17271). Briefly, seven-week-old male CD-1 mice (cohorts of eight) were rendered neutropenic by IP injection of cyclophosphamide (150 mg/kg on Day -4 to Day -2 and 100 mg/kg on Day -1). On Day -1, mice were anesthetized with a combination of xylazine/ketamine, and furs on the right hind thigh were removed by clipping with a pair of scissors followed by application of depilating gel (Veet Aloe Vera Legs & Body Hair Remover Gel Cream). After 24 h, mice were anesthetized with isoflurane, and infected with *S. aureus* ATCC 29213 or the *S. aureus* FA-resistant strain 32X-B at a concentration of $\sim 1 \times 10^6$ CFUs (in 50 μL) by injection into the thigh muscle (bicep femoris) with a 25G 5/6" needle. Infected mice were intraperitoneally treated with vehicle (85% PBS, 10% Tween, 5% DMSO), 50 mg/kg of sodium fusidate, or FA-CP (**25**) at 1, 2, and 3 h postinfection (hpi) individually in 100 μL of volume. Infected animals were monitored for myositis and lameness until euthanasia. At indicated times (24 hpi for the 50 mg/kg cohorts for the *S. aureus* ATCC 29213 infection model and 8 hpi for the 50 mg/kg cohorts for the *S. aureus* (FA-32X-B) infection model), mice were euthanized with CO₂ asphyxiation from a compressed gas source followed by cervical dislocation. Infected thigh muscle tissues were harvested and homogenized with a Omni Soft Tissue Tip Homogenizer (OMNI International) in 2 mL of sterile PBS. Bacterial burden in the tissue homogenates was determined by serial dilution plating onto tryptic soy agar.

Supplementary Material

Refer to Web version on PubMed Central for supplementary material.

ACKNOWLEDGMENTS

This work was supported by the NIH (AI136773) and the University of Illinois at Urbana–Champaign. We thank L. Li (Metabolomics Center, Roy J. Carver Biotechnology Center, UIUC) for LC-MS/MS analysis and Professor Levent Dirikolu (School of Veterinary Medicine, Louisiana State University) for the help with PK parameter calculations. M.G.C. and A.G. are members of the NIH Chemistry-Biology Interface Training Grant

(T32-GM136629). M.G.C. is also supported by the NSF Graduate Research Fellowship (NSF-GRFP). We are also grateful for the support services of the NMR and mass spectrometry facilities of the University of Illinois at Urbana-Champaign.

REFERENCES

- (1). Cassini A, Högberg LD, Plachouras D, Quattrocchi A, Hoxha A, Simonsen GS, Colomb-Cotinat M, Kretzschmar ME, Devleeschauwer B, Cecchini M, Ouakrim DA, Oliveira TC, Struelens MJ, Suetens C, Monnet DL, Strauss R, Mertens K, Struyf T, Catry B, Latour K, Ivanov IN, Dobрева EG, Tambic Andrašević A, Soprek S, Budimir A, Paphitou N, Žemlicková H, Schytte Olsen S, Wolff Sönksen U, Märtin P, Ivanova M, Lyytikäinen O, Jalava J, Coignard B, Eckmanns T, Abu Sin M, Haller S, Daikos GL, Gikas A, Tsiodras S, Kontopidou F, Tóth Á, Hajdu Á, Guólaugsson Ó, Kristinsson KG, Murchan S, Burns K, Pezzotti P, Gagliotti C, Dumpis U, Liuimiene A, Perrin M, Borg MA, de Greeff SC, Monen JCM, Koek MBG, Elstrøm P, Zabicka D, Deptula A, Hryniewicz W, Caniça M, Nogueira PJ, Fernandes PA, Manageiro V, Popescu GA, Serban RI, Schréterová E, Litvová S, Štefkovicová M, Kolman J, Klavs I, Korošec A, Aracil B, Asensio A, Pérez-Vázquez M, Billström H, Larsson S, Reilly JS, Johnson A, and Hopkins S (2019) Attributable deaths and disability-adjusted life-years caused by infections with antibiotic-resistant bacteria in the EU and the European Economic Area in 2015: a population-level modelling analysis. *Lancet Infect. Dis* 19, 56–66. [PubMed: 30409683]
- (2). Theuretzbacher U, Outtersen K, Engel A, and Karlén A (2020) The global preclinical antibacterial pipeline. *Nat. Rev. Microbiol* 18, 275–285. [PubMed: 31745331]
- (3). US Department of Health and Human Services, CDC. (2019) Antibiotic Resistance Threats in the United States 2019, US Department of Health and Human Services, CDC, Atlanta, GA.
- (4). Markwart R, Willrich N, Haller S, Noll I, Koppe U, Werner G, Eckmanns T, and Reuss A (2019) The rise in vancomycin-resistant *Enterococcus faecium* in Germany: data from the German Antimicrobial Resistance Surveillance (ARS). *Antimicrob. Resist. Infect. Control* 8, 147. [PubMed: 31485325]
- (5). Godtfredsen WO, Jahnsen S, Lorck H, Roholt K, and Tybring L (1962) Fusidic Acid: a New Antibiotic. *Nature* 193, 987–987. [PubMed: 13899435]
- (6). Tanaka N, Kinoshita T, and Masukawa H (1968) Mechanism of protein synthesis inhibition by fusidic acid and related antibiotics. *Biochem. Biophys. Res. Commun* 30, 278–283. [PubMed: 4296678]
- (7). Fernandes P (2016) Fusidic Acid: A Bacterial Elongation Factor Inhibitor for the Oral Treatment of Acute and Chronic Staphylococcal Infections. *Cold Spring Harbor Perspect. Med* 6, a025437–a025437.
- (8). Jones RN, Castanheira M, Rhomberg PR, Woosley LN, and Pfaller MA (2010) Performance of fusidic acid (CEM-102) susceptibility testing reagents: broth microdilution, disk diffusion, and Etest methods as applied to *Staphylococcus aureus*. *J. Clin. Microbiol* 48, 972–976. [PubMed: 20053856]
- (9). Cempra. Cempra's Fusidic Acid Achieves Primary Endpoint in Phase 3 Study of ABSSSI, <http://ir.melinta.com/static-files/d621fa2f-d0d4-4fc3-833f-a64286cfb7ed> (accessed November 11, 2020).
- (10). Melinta Therapeutics. Cempra, Inc. Receives U.S. Orphan Drug Designation for Taksta(TM) for Treatment of Prosthetic Joint Infections, <http://ir.melinta.com/news-releases/news-release-details/cempra-inc-receives-us-orphan-drug-designation-takstatm> (accessed November 11, 2020).
- (11). Nagaev I, Björkman J, Andersson DI, and Hughes D (2001) Biological cost and compensatory evolution in fusidic acid-resistant *Staphylococcus aureus*. *Mol. Microbiol* 40, 433–439. [PubMed: 11309125]
- (12). Silver LL (2017) The Antibiotic Future. *Top. Med. Chem* 25, 31–67.
- (13). Silver LL (2016) Appropriate Targets for Antibacterial Drugs. *Cold Spring Harbor Perspect. Med.* 6, a030239.
- (14). Tomlinson JH, Kalverda AP, and Calabrese AN (2020) Fusidic acid resistance through changes in the dynamics of the drug target. *Proc. Natl. Acad. Sci. U. S. A* 117, 25523. [PubMed: 32999060]

- (15). Abouelfetouh A, Kassem M, Naguib M, and El-Nakeeb M (2017) Investigation and Treatment of Fusidic Acid Resistance Among Methicillin-Resistant Staphylococcal Isolates from Egypt. *Microb. Drug Resist* 23, 8–17. [PubMed: 27228193]
- (16). Von Daehne W, Godtfredsen WO, and Rasmussen PR (1979) Structure-Activity Relationships in Fusidic Acid-Type Antibiotics. *Adv. Appl. Microbiol* 25, 95–146. [PubMed: 397741]
- (17). Duvold T, Sørensen MD, Björkling F, Henriksen AS, and Rastrup-Andersen N (2001) Synthesis and Conformational Analysis of Fusidic Acid Side Chain Derivatives in Relation to Antibacterial Activity. *J. Med. Chem* 44, 3125–3131. [PubMed: 11543681]
- (18). Janssen G, and Vanderhaeghe H (1967) Modification of the Side Chain of Fusidic Acid (Ramyacin). *J. Med. Chem* 10, 205–208. [PubMed: 4962805]
- (19). Bodley JW, and Godtfredsen WO (1972) Studies on translocation XI: Structure-function relationships of the fusidane-type antibiotics. *Biochem. Biophys. Res. Commun* 46, 871–877. [PubMed: 5057912]
- (20). Willie GR, Richman N, Godtfredsen WO, and Bodley JW (1975) Translocation. XV. Characteristics of and structural requirements for the interaction of 24,25-dihydrofusidic acid with ribosome. elongation factor G complexes. *Biochemistry* 14, 1713–1718. [PubMed: 1092341]
- (21). Kaur G, Pavadai E, Wittlin S, and Chibale K (2018) 3D-QSAR Modeling and Synthesis of New Fusidic Acid Derivatives as Antiplasmodial Agents. *J. Chem. Inf. Model* 58, 1553–1560. [PubMed: 30040885]
- (22). Wu P-P, He H, Hong WD, Wu T-R, Huang G-Y, Zhong Y-Y, Tu B-R, Gao M, Zhou J, Zhao S-Q, Li D-L, Xu X-T, Sheng Z-J, Ward SA, O'Neill PM, and Zhang K (2018) The biological evaluation of fusidic acid and its hydrogenation derivative as antimicrobial and anti-inflammatory agents. *Infect. Drug Resist* 11, 1945–1957. [PubMed: 30498366]
- (23). Riber D, Venkataramana M, Sanyal S, and Duvold T (2006) Synthesis and Biological Evaluation of Photoaffinity Labeled Fusidic Acid Analogues. *J. Med. Chem* 49, 1503–1505. [PubMed: 16509567]
- (24). Dauben WG, Kessel CR, Kishi M, Somei M, Tada M, and Guillerme D (1982) A formal total synthesis of fusidic acid. *J. Am. Chem. Soc* 104, 303–305.
- (25). Ireland RE, Giger R, and Kamata S (1977) Studies on the total synthesis of steroidal antibiotics. 3. Generation and correlation of tetracyclic derivatives from the degradation of fusidic acid and total synthesis. *J. Org. Chem* 42, 1276–1282. [PubMed: 845710]
- (26). Kaur G, Singh K, Pavadai E, Njoroge M, Espinoza-Moraga M, De Kock C, Smith PJ, Wittlin S, and Chibale K (2015) Synthesis of fusidic acid bioisosteres as antiplasmodial agents and molecular docking studies in the binding site of elongation factor-G. *MedChemComm* 6, 2023–2028.
- (27). Hill CK, and Hartwig JF (2017) Site-selective oxidation, amination and epimerization reactions of complex polyols enabled by transfer hydrogenation. *Nat. Chem* 9, 1213–1221. [PubMed: 29168493]
- (28). Njoroge M, Kaur G, Espinoza-Moraga M, Wasuna A, Dziwornu GA, Seldon R, Taylor D, Okombo J, Warner DF, and Chibale K (2019) Semisynthetic Antimycobacterial C-3 Silicate and C-3/C-21 Ester Derivatives of Fusidic Acid: Pharmacological Evaluation and Stability Studies in Liver Microsomes, Rat Plasma, and Mycobacterium tuberculosis culture. *ACS Infect. Dis* 5, 1634–1644. [PubMed: 31309823]
- (29). Suchkova GS, Lokshin GB, Kuzovkov AD, and Chernyshev AI (1979) Oxidation of fusidic acid. *Chem. Nat. Compd* 15, 54–56.
- (30). Espinoza-Moraga M, Singh K, Njoroge M, Kaur G, Okombo J, De Kock C, Smith PJ, Wittlin S, and Chibale K (2017) Synthesis and biological characterisation of ester and amide derivatives of fusidic acid as antiplasmodial agents. *Bioorg. Med. Chem. Lett* 27, 658–661. [PubMed: 28012840]
- (31). Dziwornu GA, Kamunya S, Ntsabo T, and Chibale K (2019) Novel antimycobacterial C-21 amide derivatives of the antibiotic fusidic acid: synthesis, pharmacological evaluation and rationalization of media-dependent activity using molecular docking studies in the binding site of human serum albumin. *MedChemComm* 10, 961–969. [PubMed: 31303994]

- (32). Strydom N, Kaur G, Dziwornu GA, Okombo J, Wiesner L, and Chibale K (2020) Pharmacokinetics and Organ Distribution of C-3 Alkyl Esters as Potential Antimycobacterial Prodrugs of Fusidic Acid. *ACS Infect. Dis* 6, 459–466. [PubMed: 32011859]
- (33). Tanabe M, Yasuda DM, and Peters RH (1977) Partial synthesis of fusidic acid. *Tetrahedron Lett* 18, 1481–1484.
- (34). Krakower GW, Van Dine HA, Diassi PA, and Bacso I (1967) Transformations of fusidic acid. III. 17-Oxa-4.alpha.,8,-14-trimethyl-D-homo-18-norandrostanes. *J. Org. Chem* 32, 184–191. [PubMed: 6035700]
- (35). CLSI. (2018) *Methods for Dilution Antimicrobial Susceptibility Tests for Bacteria That Grow Aerobically*, 11th ed., Clinical and Laboratory Standards Institute, Wayne, PA.
- (36). Gao Y-G, Selmer M, Dunham CM, Weixlbaumer A, Kelley AC, and Ramakrishnan V (2009) The structure of the ribosome with elongation factor G trapped in the posttranslocational state. *Science* 326, 694–699. [PubMed: 19833919]
- (37). Zhao SW, Panpan, Zhang K, Hong W, Jiang Z, Cui X, Cheng A, and Qin J Fusidic acid chemically modified compounds, and preparation method and application thereof, CN 105924488A, 9. 7, 2016.
- (38). Ibrahim A-RS, Elokely KM, Ferreira D, and Ragab AE (2018) Microbial Oxidation of the Fusidic Acid Side Chain by *Cunninghamella echinulata*. *Molecules* 23, 970.
- (39). Biedenbach DJ, Rhomberg PR, Mendes RE, and Jones RN (2010) Spectrum of activity, mutation rates, synergistic interactions, and the effects of pH and serum proteins for fusidic acid (CEM-102). *Diagn. Microbiol. Infect. Dis* 66, 301–307. [PubMed: 20159376]
- (40). Laue H, Valensise T, Seguin A, Hawser S, Lociuro S, and Islam K (2007) Effect of human plasma on the antimicrobial activity of iclaprim in vitro. *J. Antimicrob. Chemother* 60, 1388–1390. [PubMed: 17951265]
- (41). O'Neill AJ, Bostock JM, Morais Moita A, and Chopra I (2002) Antimicrobial activity and mechanisms of resistance to cephalosporin P1, an antibiotic related to fusidic acid. *J. Antimicrob. Chemother* 50, 839–848. [PubMed: 12461002]
- (42). Besier S, Ludwig A, Brade V, and Wichelhaus TA (2003) Molecular analysis of fusidic acid resistance in *Staphylococcus aureus*. *Mol. Microbiol* 47, 463–469. [PubMed: 12519196]
- (43). Chen W, He C, Yang H, Shu W, Cui Z, Tang R, Zhang C, and Liu Q (2020) Prevalence and molecular characterization of methicillin-resistant *Staphylococcus aureus* with mupirocin, fusidic acid and/or retapamulin resistance. *BMC Microbiol* 20, 183. [PubMed: 32600253]
- (44). Chen C-M, Huang M, Chen H-F, Ke S-C, Li C-R, Wang J-H, and Wu L-T (2011) Fusidic acid resistance among clinical isolates of methicillin-resistant *Staphylococcus aureus* in a Taiwanese hospital. *BMC Microbiol* 11, 98–98. [PubMed: 21569422]
- (45). Norström T, Lannergård J, and Hughes D (2007) Genetic and Phenotypic Identification of Fusidic Acid-Resistant Mutants with the Small-Colony-Variant Phenotype in *Staphylococcus aureus*. *Antimicrob. Agents Chemother* 51, 4438. [PubMed: 17923494]
- (46). O'Neill AJ, McLaws F, Kahlmeter G, Henriksen AS, and Chopra I (2007) Genetic basis of resistance to fusidic acid in staphylococci. *Antimicrob. Agents Chemother* 51, 1737–1740. [PubMed: 17325218]
- (47). Still JG, Clark K, Degenhardt TP, Scott D, Fernandes P, and Gutierrez MJ (2011) Pharmacokinetics and Safety of Single, Multiple, and Loading Doses of Fusidic Acid in Healthy Subjects. *Clin. Infect. Dis* 52, S504–S512. [PubMed: 21546627]
- (48). Godtfredsen WO, and Vangedal S (1966) On the metabolism of fusidic acid in man. *Acta Chem. Scand* 20, 1599–1607. [PubMed: 5966866]
- (49). Murphy TM, Little S, Wu R, Slee A, and Fernandes P Assessment of In Vivo Activity of CEM-102 (Fusidic Acid) in Murine Infection Models, <http://melinta.com/wp-content/uploads/alltime/pdf/c/Assessment%20of%20In%20Vivo%20Activity%20of%20CEM-102%20in%20Murine.pdf> (accessed November 11, 2020).
- (50). Chen Y, Koripella RK, Sanyal S, and Selmer M (2010) *Staphylococcus aureus* elongation factor G—structure and analysis of a target for fusidic acid. *FEBS J* 277, 3789–803. [PubMed: 20718859]

- (51). Cox G, Thompson GS, Jenkins HT, Peske F, Savelsbergh A, Rodnina MV, Wintermeyer W, Homans SW, Edwards TA, and O'Neill AJ (2012) Ribosome clearance by FusB-type proteins mediates resistance to the antibiotic fusidic acid. *Proc. Natl. Acad. Sci. U. S. A* 109, 2102. [PubMed: 22308410]
- (52). Oefner C, Bandera M, Haldimann A, Laue H, Schulz H, Mukhija S, Parisi S, Weiss L, Lociuro S, and Dale GE (2009) Increased hydrophobic interactions of iclaprim with *Staphylococcus aureus* dihydrofolate reductase are responsible for the increase in affinity and antibacterial activity. *J. Antimicrob. Chemother* 63, 687–698. [PubMed: 19211577]
- (53). Purnapatre KP, Rao M, Pandya M, Khanna A, Chaira T, Bambal R, Upadhyay DJ, and Masuda N (2018) In Vitro and In Vivo Activities of DS86760016, a Novel Leucyl-tRNA Synthetase Inhibitor for Gram-Negative Pathogens. *Antimicrob. Agents Chemother* 62, e01987–17. [PubMed: 29437618]
- (54). Sulavik MC, Houseweart C, Cramer C, Jiwani N, Murgolo N, Greene J, DiDomenico B, Shaw KJ, Miller GH, Hare R, and Shimer G (2001) Antibiotic Susceptibility Profiles of *Escherichia coli* Strains Lacking Multidrug Efflux Pump Genes. *Antimicrob. Agents Chemother* 45, 1126. [PubMed: 11257026]

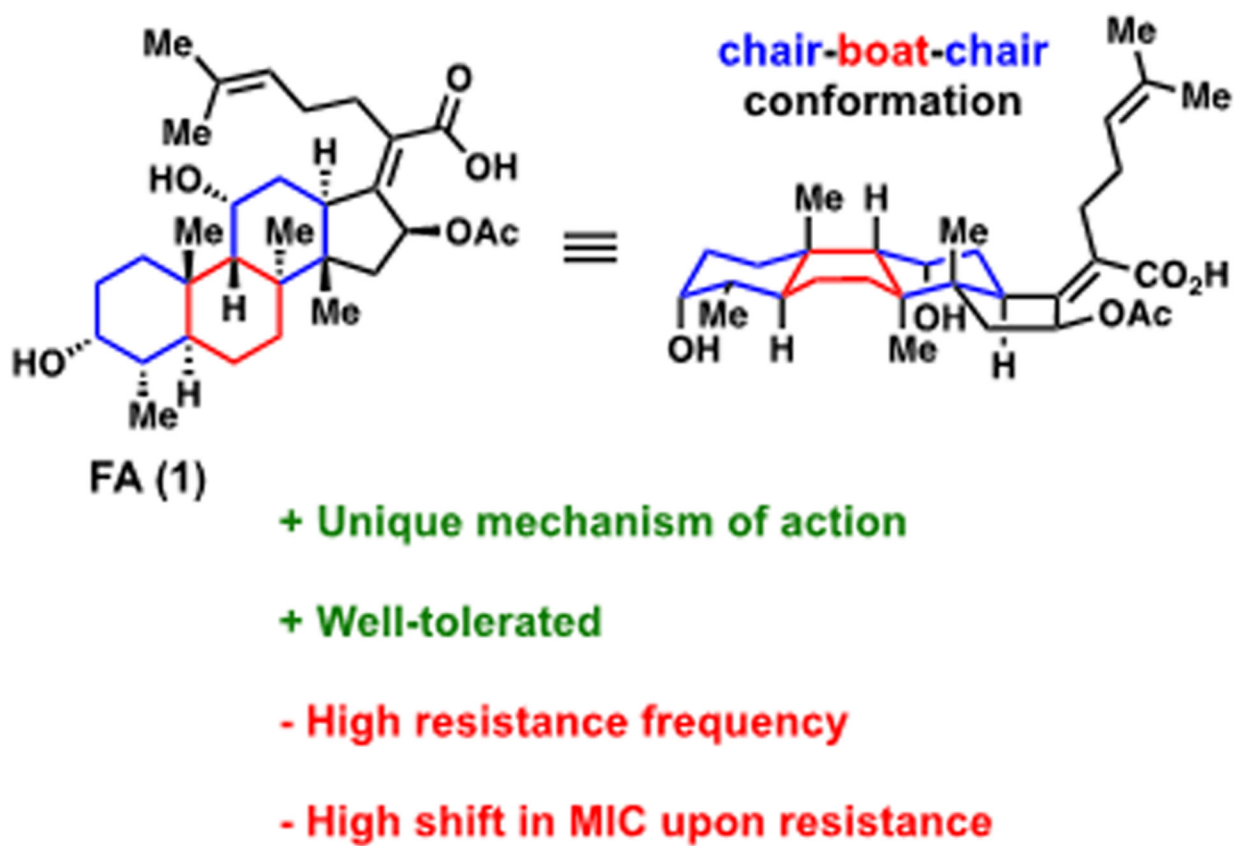
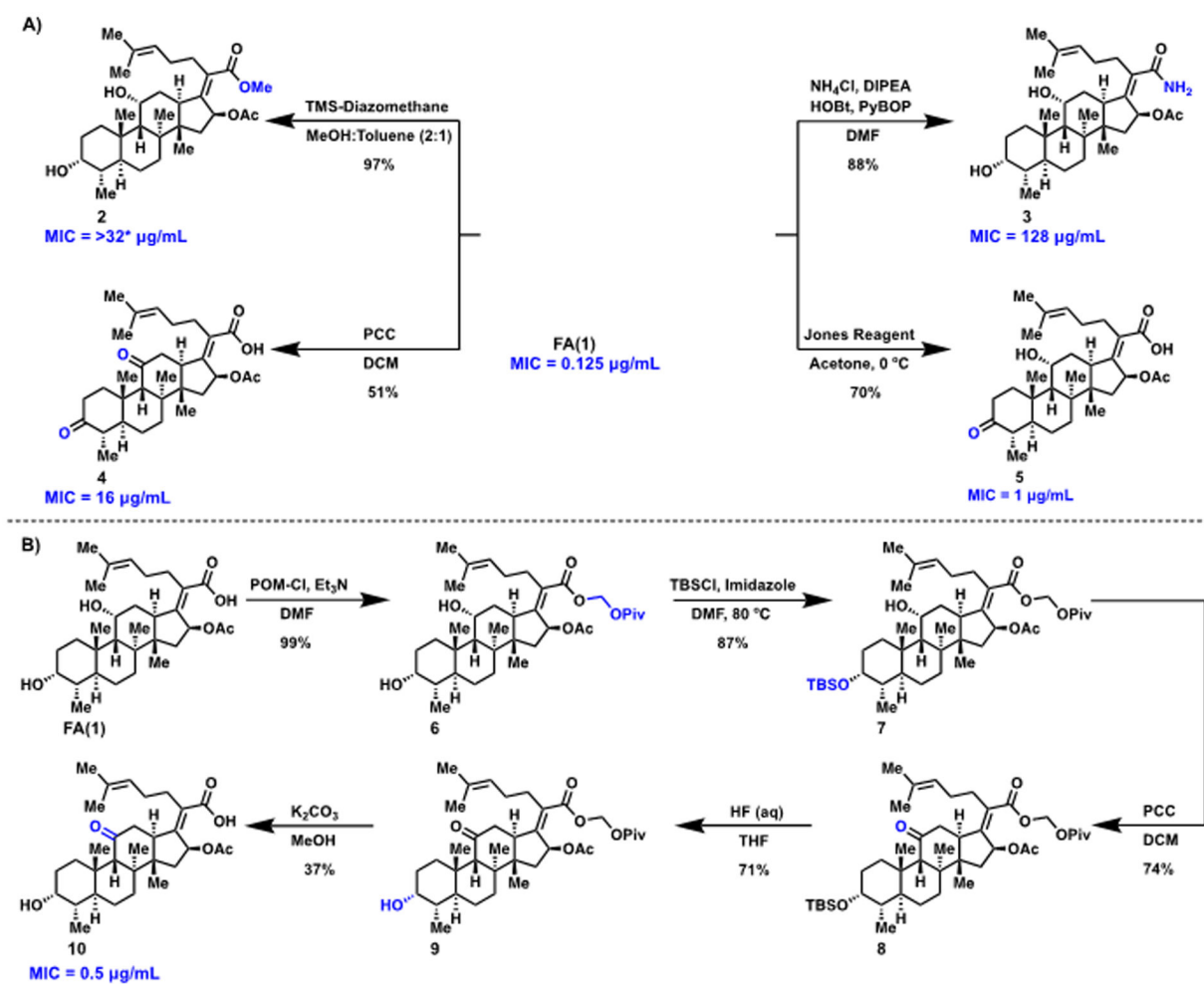


Figure 1.
Structure of fusidic acid (FA), with some of its properties.



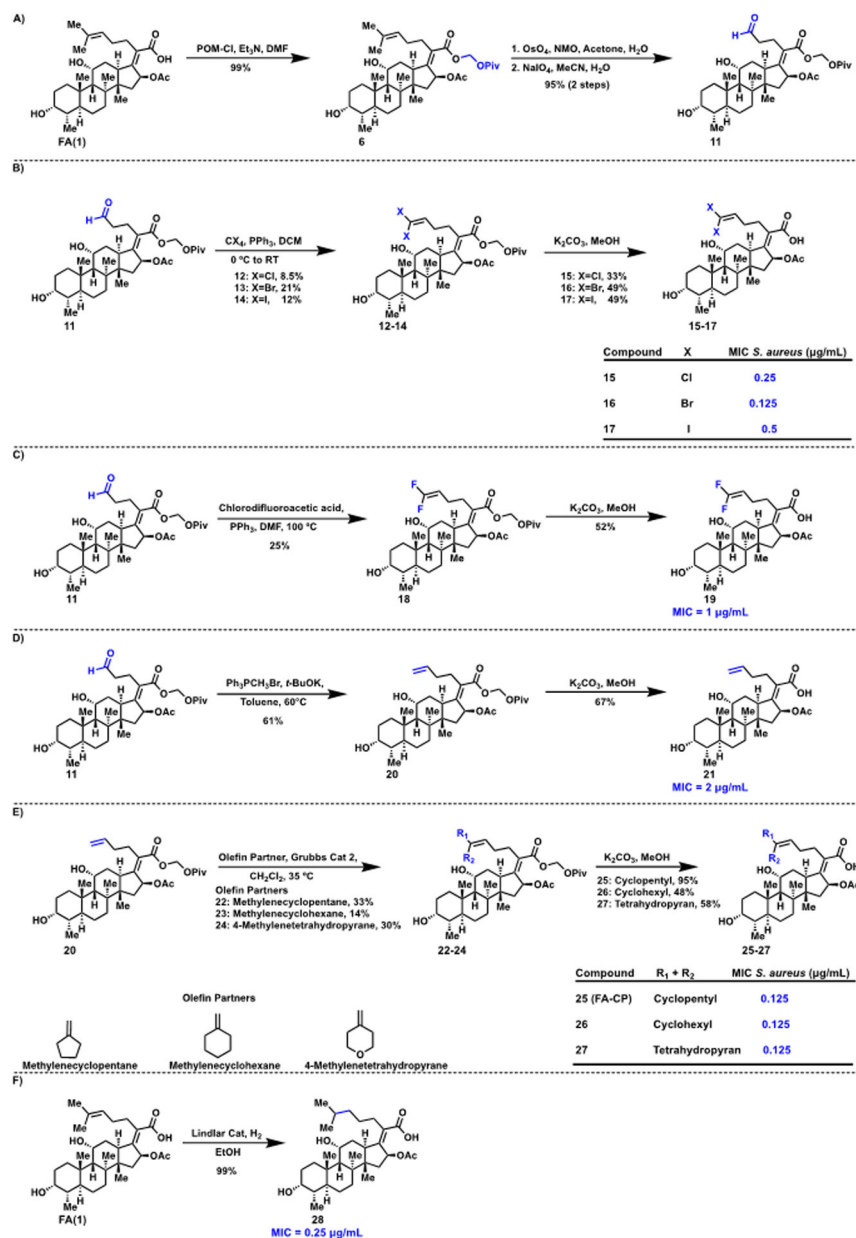


Figure 3. (A) Synthesis of aliphatic aldehyde derivative of FA. (B) Construction of halogenated side chain analogues of FA. (C) Generation of fluorinated side chain analogue of FA. (D) Synthesis of an FA analogue with a terminal olefin side chain. (E) Synthesis of cyclic side chain derivatives of FA. (F) Formation of saturated side chain derivative of FA. MICs determined using CLSI guidelines, against *S. aureus* ATCC 29213, $n = 3$.

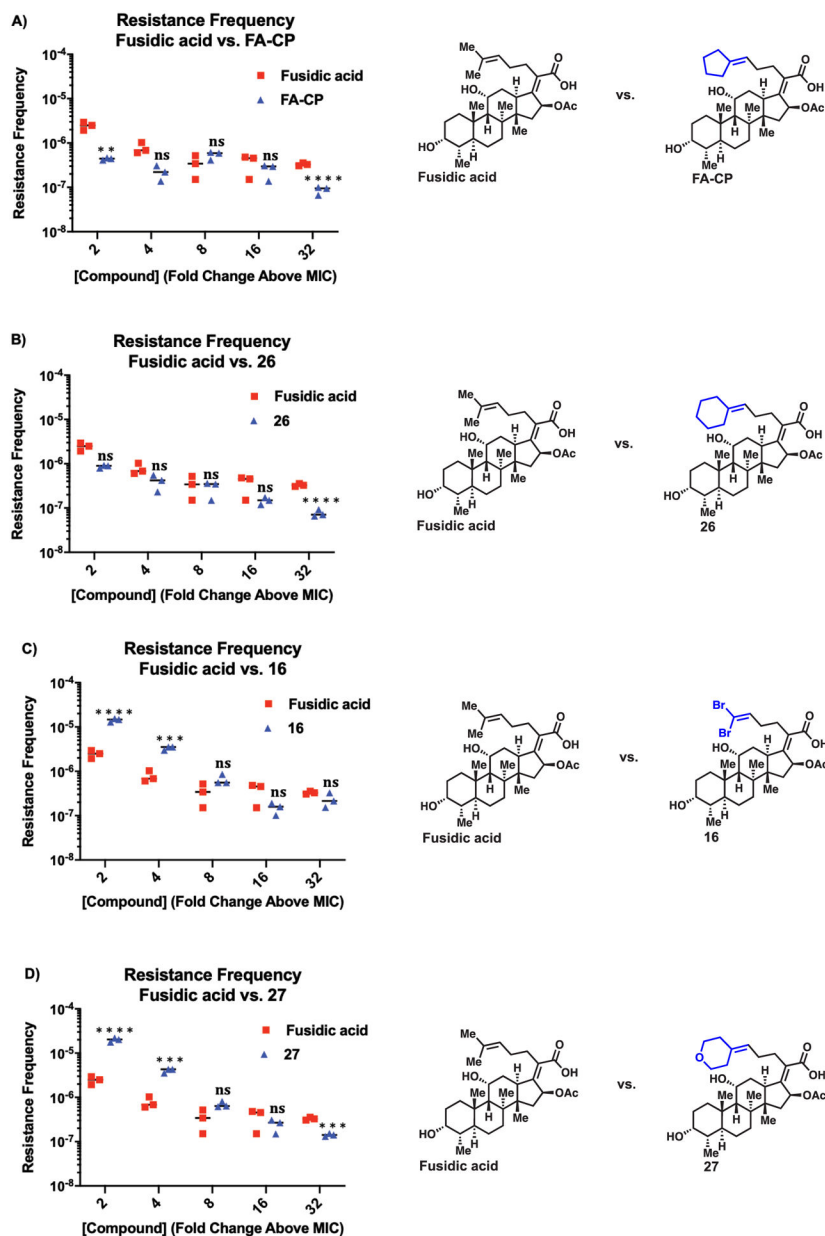


Figure 4. (A) Resistance frequency of FA-CP. (B) Resistance frequency of compound 26. (C) Resistance frequency of compound 16. (D) Resistance frequency of compound 27. Resistance frequency of FA and equipotent analogues was determined in *S. aureus* ATCC 29213. FA data is the same in all four experiments. Error is SEM, $n = 3$. NS = not significant, ** $p < 0.01$, *** $p < 0.001$, and **** $p < 0.0001$.

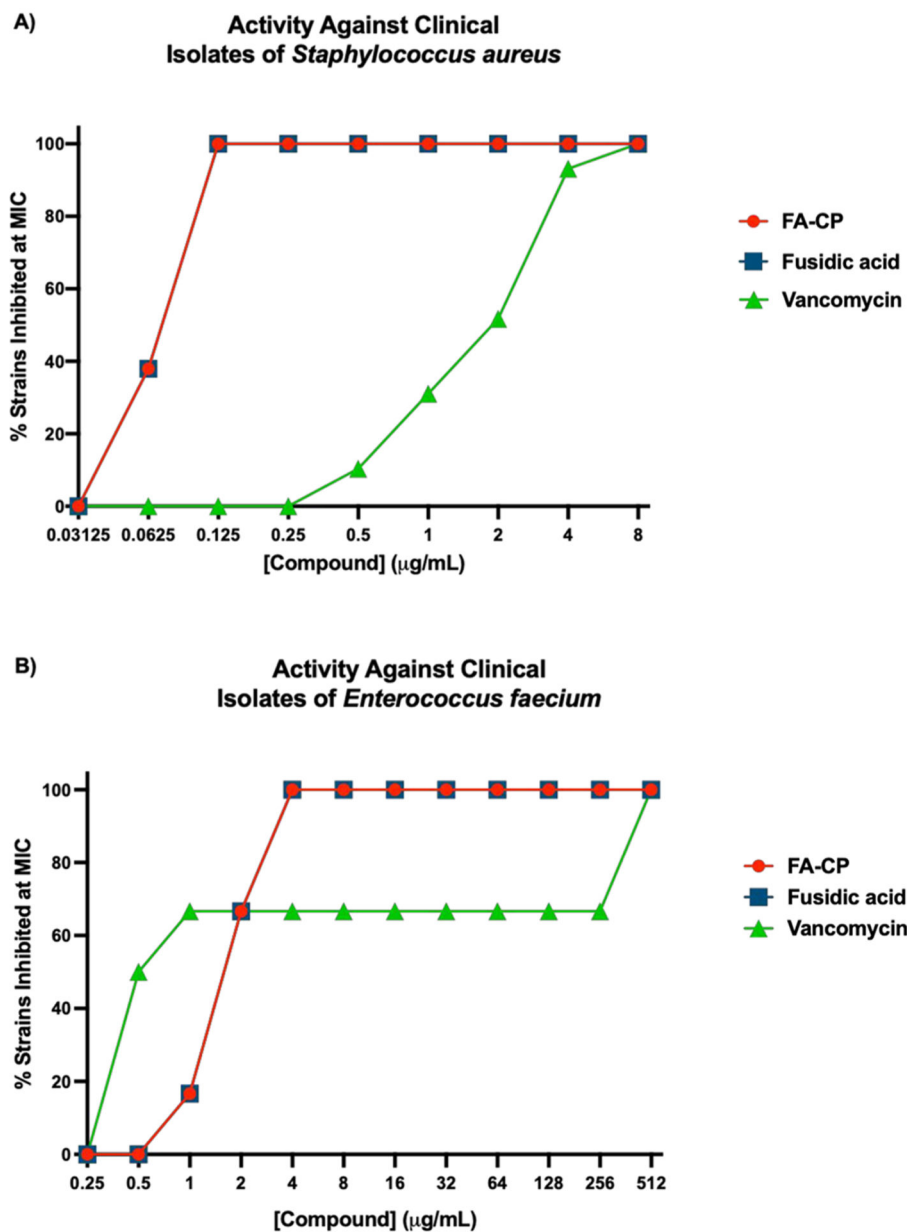


Figure 5. (A) Activity against 29 clinical isolates of *S. aureus*. (B) Activity against six different clinical isolates of *E. faecium*. MICs determined using CLSI guidelines, $n = 3$. See Tables S4–S6 for a list of resistance genes in clinical isolate panels. A full listing of this MIC data is in Tables S5 and S6.

Fusidic acid		FA-CP	
Parameter	Estimate	Parameter	Estimate
AUC	561,683 min*ng/ml	AUC	701,474 min*ng/ml
K10_HL	31.2 min	K10_HL	19.0 min
CL_F	89.0 ml/min/kg	CL_F	71.3 ml/min/kg
Tmax	5.4 min	Tmax	26.4 min
Cmax	11,056.7 ng/ml	Cmax	9,757.5 ng/ml

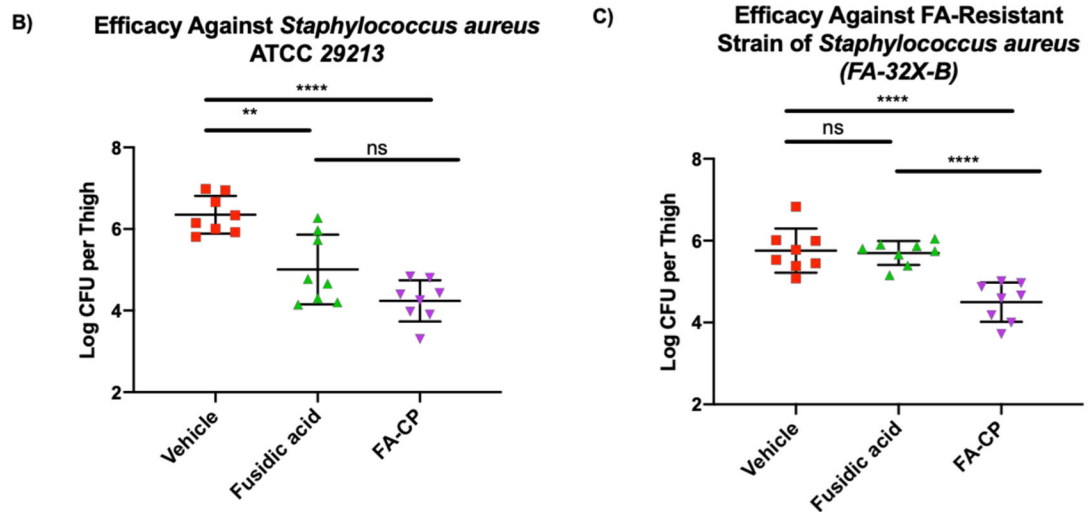
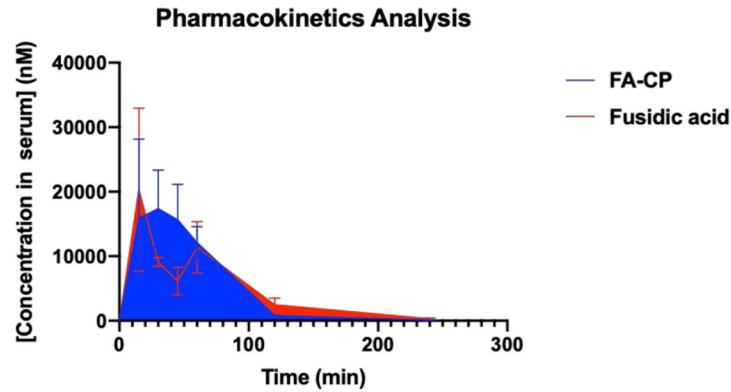


Figure 6.

(A) Pharmacokinetic analysis of fusidic acid and FA-CP. C57BL/6 mice were treated with 50 mg/kg of fusidic acid or FA-CP via intraperitoneal injection, with three mice per time point (0, 15, 30, 45, 60, 120, and 240 min). After the stated time points, mice were sacrificed, and the serum concentrations of fusidic acid or FA-CP were determined by liquid chromatography–tandem mass spectrometry (LC–MS/MS). The data are illustrated as the mean, and error bars represent the standard error. The pharmacokinetic parameters illustrated above were calculated with a one-compartment model using a nonlinear regression program (Phoenix WinNonlin Version 8.1, Certara USA Inc., Princeton, NJ, USA). (B) *S. aureus* ATCC 29213 neutropenic thigh infection burden study. CD-1 mice were first rendered neutropenic with cyclophosphamide. Mice were injected on Day -4 to

Day -2 with 150 mg/kg and on Day -1 with 100 mg/kg of cyclophosphamide, respectively. Acute thigh infections initiated in CD-1 mice with *S. aureus* ATCC 29213 (8.9×10^5 colony forming units (CFU) mouse⁻¹ via intramuscular injection) were treated with vehicle, fusidic acid, and FA-CP (eight mice per group) at 1, 2, and 3 h postinfection (50 mg/kg via intraperitoneal injection), and the bacterial burden was evaluated at 24 h postinfection. (C) *S. aureus* (FA-32X-B) neutropenic thigh infection study. CD-1 mice were first rendered neutropenic with cyclophosphamide as described above. Acute thigh infections initiated in CD-1 mice with *S. aureus* (FA-32X-B) (1.08×10^6 CFU mouse⁻¹ via intramuscular injection) were treated with vehicle, fusidic acid, and FA-CP (eight mice per group) at 1, 2, and 3 h postinfection (50 mg/kg via intraperitoneal injection), and the bacterial burden was evaluated at 8 h postinfection. Drugs were formulated with 5% DMSO, 10% Tween 20, 85% PBS immediately before injection. The data is shown as means \pm s.d., and statistical significance was determined by one-way ANOVA with Tukey's multiple comparisons. NS indicates not significant ($P > 0.05$), ** $P < 0.01$, **** $P < 0.0001$.

Table 1.

Observed Mutations in the EF-G Protein (Encoded by *fusA*) and MIC Values for FA and FA-CP at 32X the MIC in *S. aureus* ATCC 29213

strains resistant to FA	EF-G mutation	MIC for FA	strains resistant to FA-CP	EF-G mutation	MIC for FA-CP
FA-32X-1	H457Y	128	FA-CP-32X-1	H457Y	32
FA-32X-2	T436I	8	FA-CP-32X-2	H457Y	64
FA-32X-3	H457Y	128	FA-CP-32X-3	H457Y	64
FA-32X-4	H457N	256	FA-CP-32X-4	H457Y	32
FA-32X-5	F88L	256	FA-CP-32X-5	H457Y	64
FA-32X-6	T436I	16	FA-CP-32X-6	H457Y	64
FA-32X-7	H457Y	128	FA-CP-32X-7	H457Y	64
FA-32X-8	H457Y	128	FA-CP-32X-8	H457Y	64
FA-32X-9	F88L	256	FA-CP-32X-9	H457Y	32
FA-32X-10	H457Y	128	FA-CP-32X-10	D434N	32
FA-32X-11	F88L	256	FA-CP-32X-11	H457Y	32
FA-32X-12	H457Y	128	FA-CP-32X-12	D434N	32
FA-32X-13	H457Y	128	FA-CP-32X-13	H457Y	64
FA-32X-14	H457Y	128	FA-CP-32X-14	H457Y	32
FA-32X-15	H457Y	128	FA-CP-32X-15	H457Y	64
FA-32X-16	F88L	256	FA-CP-32X-16	F88L	64
FA-32X-17	H457N	256	FA-CP-32X-17	F88L	64
FA-32X-18	D434N	256	FA-CP-32X-18	H457Y	64
FA-32X-19	H457Y	128	FA-CP-32X-19	H457Y	32
FA-32X-20	H457Y	128	FA-CP-32X-20	H457Y	32

Table 2.MIC Values for FA and FA-CP against 11 Different FA-Resistant Strains of *S. aureus* ATCC 29213^a

strains resistant to FA	EF-G mutation	MIC for FA	MIC for FA-CP
FA-4X-A	T385N	8	2
FA-4X-B	T385N	8	2
FA-8X-A	T385N	8	2
FA-8X-B	R464L	16	8
FA-16X-A	H457Y	128	64
FA-32X-A	F88L	256	128
FA-32X-B	P406L	32	4
FA-32X-C	H457L	256	128
FA-32X-D	T436I	8	2
FA-32X-E	H457N	256	128
FA-32X-F	D434N	256	32

^aFA-resistant strains were generated at 4X ($n = 2$), 8X ($n = 2$), 16X ($n = 1$), or 32X ($n = 6$) the MIC as indicated. MICs determined using CLSI guidelines, $n = 3$.